

## Mass measurements of relativistic projectile fragments in the storage ring ESR

T RADON<sup>1</sup>, H GEISSEL<sup>1</sup>, F ATTALLAH<sup>1</sup>, K BECKERT<sup>1</sup>, F BOSCH<sup>1</sup>,  
A DOLINSKIY<sup>1</sup>, H EICKHOFF<sup>1</sup>, M FALCH<sup>2</sup>, B FRAN CZAK<sup>1</sup>, B FRANZKE<sup>1</sup>,  
Y FUJITA<sup>3</sup>, M HAUSMANN<sup>1</sup>, M HELLSTRÖM<sup>1</sup>, F HERFURTH<sup>1</sup>, TH KERSCHER<sup>2</sup>,  
O KLEPPER<sup>1</sup>, H-J KLUGE<sup>1</sup>, C KOZHUHAROV<sup>1</sup>, YU LITVINOV<sup>4</sup>, K E G LÖBNER<sup>2</sup>,  
G MÜNZENBERG<sup>1</sup>, F NOLDEN<sup>1</sup>, YU NOVIKOV<sup>4</sup>, Z PATYK<sup>5</sup>, W QUINT<sup>1</sup>,  
H REICH<sup>1</sup>, C SCHEIDENBERGER<sup>1</sup>, B SCHLITT<sup>1</sup>, J STADLMANN<sup>6</sup>, M STECK<sup>1</sup>,  
K SÜMMERER<sup>1</sup>, L VERMEEREN<sup>1</sup>, M WINKLER<sup>1</sup>, TH WINKLER<sup>1</sup> and  
H WOLLNIK<sup>6</sup>

<sup>1</sup>Gesellschaft für Schwerionenforschung mbH, Planckstraße 1, D-64291 Darmstadt, Germany

<sup>2</sup>Sektion für Physik, LMU München, Am Coulombwall, D-85748 Garching, Germany

<sup>3</sup>Department of Physics, Osaka University, Toyonaka, Osaka 560, Japan

<sup>4</sup>St. Petersburg Nuclear Physics Institute, Gatchina 188350, Russia

<sup>5</sup>Soltan Institute for Nuclear Studies, 00-681 Warsaw, Poland

<sup>6</sup>II. Physikalisches Institut, JLU Gießen, Heinrich-Buff-Ring 16, D-35392 Gießen, Germany

**Abstract.** Two experimental methods of measuring masses of exotic nuclei in the storage ring ESR are presented. Bismuth and nickel fragments were produced via projectile fragmentation, separated and investigated with the combination of the fragment separator FRS and the ESR: (i) Direct mass measurements of relativistic projectile fragments were performed using Schottky mass spectrometry (SMS), i.e., exotic nuclei were stored and cooled in the ESR. Applying electron cooling, the relative velocity spread of circulating low intensity beams can be reduced below  $10^{-6}$ . Under this condition a mass resolving power of up to  $m/\Delta m = 6.5 \cdot 10^5$  (FWHM) was achieved in a recent measurement. Previously unknown masses of more than 100 neutron-deficient isotopes have been measured in the range of  $60 \leq Z \leq 84$ . Using known  $Q_\alpha$  values the area of known masses could be extended to more exotic nuclei and to higher proton numbers. The results are compared with mass models and extrapolations of experimental values. In a second experiment with  $^{209}\text{Bi}$  projectiles the area of the measured masses was extended to lower proton numbers. Due to various improvements at the ESR the precision of the measurements could be raised. (ii) Exotic nuclei with half-lives shorter than the time needed for SMS (present limit:  $T_{1/2} \approx 5$  sec) can be investigated by time-of-flight measurements whereby the ESR is operated in the isochronous mode. This novel experimental technique has been successfully applied in first measurements with nickel and neon fragments where a mass resolving power of  $m/\Delta m = 1.5 \cdot 10^5$  (FWHM) was achieved.

**Keywords.** Mass measurements; storage ring; Schottky spectroscopy; isochronous mode.

**PACS No.** 21.10.Dr; 27.80.+w; 29.20.Dh

## 1. Introduction

The mass of a nucleus is its most fundamental property as it reflects all forces between the nucleons. By now only 1600 atomic masses are known whereas the existence of more than 2500 nuclei is established. Nuclei with known masses can be found in or near the valley of  $\beta$ -stability (see figure 1).

However, the study of masses far off stability, where nuclear models have large uncertainties, will contribute more to an improved knowledge of nuclear binding and structure. Here the masses of nuclei are most important for the understanding of astrophysical processes ( $r$ -,  $s$ -,  $rp$ -path). Recent review articles [1–3] present the progress of atomic mass measurements.

The unique combination of the fragment separator FRS [4] and the experimental storage ring ESR [5] gives excellent conditions to perform mass measurements of relativistic exotic nuclei. We performed measurements on the neutron deficient part of the lead region [6,7]. This area was mainly chosen due to the possibility to connect members of  $\alpha$ -chains linked by precise  $Q_\alpha$  values to the backbone of known masses [6] in order to cover nuclei at the proton dripline. Another motivation was to measure masses of refractory elements ( $72 \leq Z \leq 78$ ) which cannot be produced by ISOL-techniques. Including  $\alpha$ -chains we were able to cover a large number of elements reaching from proton numbers of about 60 up to uranium. An overview of the mass surface covered by our mass measurements with  $^{209}\text{Bi}$  projectiles is shown in figure 2. The isotopes with known masses before our experiments as well as those which were measured in 1995 and 1997 for the first time are indicated in the chart of nuclides 6. In the experiment performed in 1997 we extended the measured

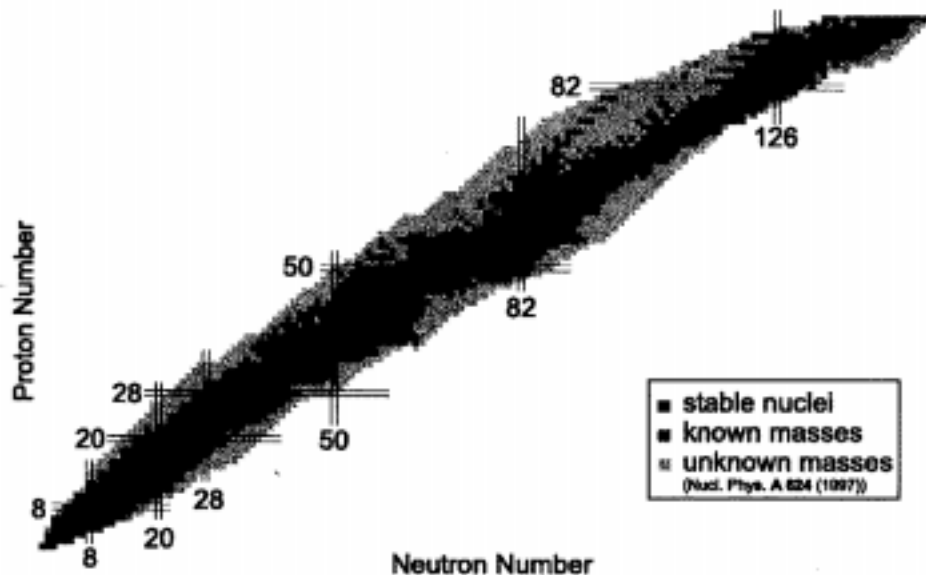
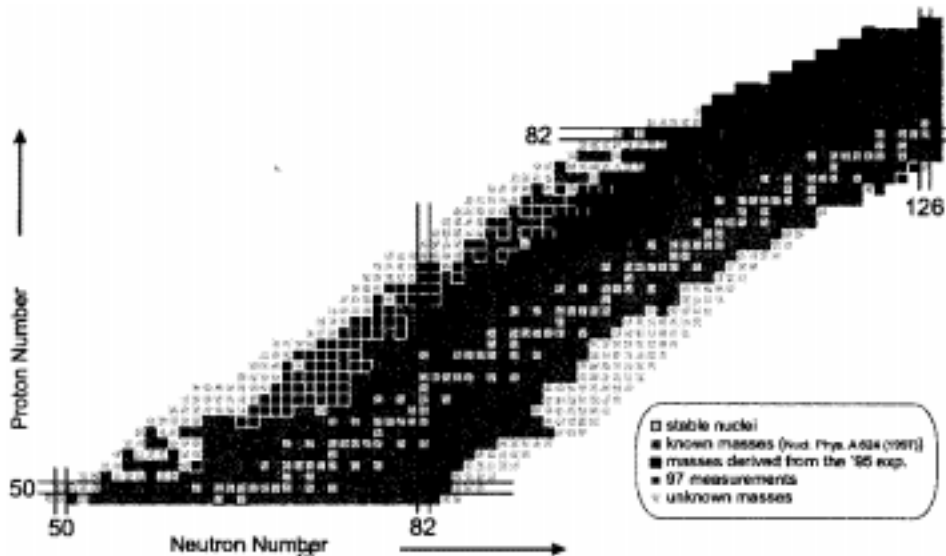


Figure 1. Chart of nuclei showing known and unknown masses up to  $Z = 94$ .



**Figure 2.** Range of FRS-ESR mass measurements covered in experiments with  $^{209}\text{Bi}$  projectile fragments in 1995 and 1997. In the latter experiment we extended the measured mass surface down to cesium and also to neutron-rich fragments near the shell closures at  $Z = 82$  and  $N = 126$ . The marked areas of our studies represent the previously unknown masses only [7].

mass surface to smaller  $Z$  values down to tin and also to neutron-rich fragments near the shell closures at  $Z = 82$  and  $N = 126$ .

## 2. Two ways of mass measurements at the SIS-FRS-ESR facility

Stable beams of relativistic heavy ions provided by the synchrotron SIS [8] are converted into exotic nuclei by nuclear collisions in the production target at the entrance of the spectrometer FRS. The FRS [9] separates the fragments in flight and injects them into the ESR for precise mass determination, performed by measuring the revolution frequency of the stored ions. The ESR is equipped with an electron cooler [10] and can store ions in the range of  $(0.5 \leq B\rho \leq 10) \text{ Tm}$ . The storage time of the circulating nuclei ( $\tau_{\text{st}}$ ) is limited by atomic collisions with atoms of the residual gas (pressure  $\leq 10^{-10}$  mbar) and with the electrons of the cooler.  $\tau_{\text{st}}$  can range from hours up to days depending on the velocity and the charge state of the stored ions. The phase-space density of the stored ions can be drastically reduced by electron cooling, e.g., the relative velocity spread of a low-intensity cooled beam can be less than  $10^{-6}$ .

Two methods are employed to perform precise mass measurements of stored ions circulating in the ESR: (i) Mass spectrometry using cooled ion beams [6,11]. (ii) Mass spectrometry of hot fragments operating the ESR in the isochronous mode. Both principles can be easily understood by the first-order relation between the mass  $m$ , the revolution frequency  $f$ , and the velocity  $v$  (see figure 3).

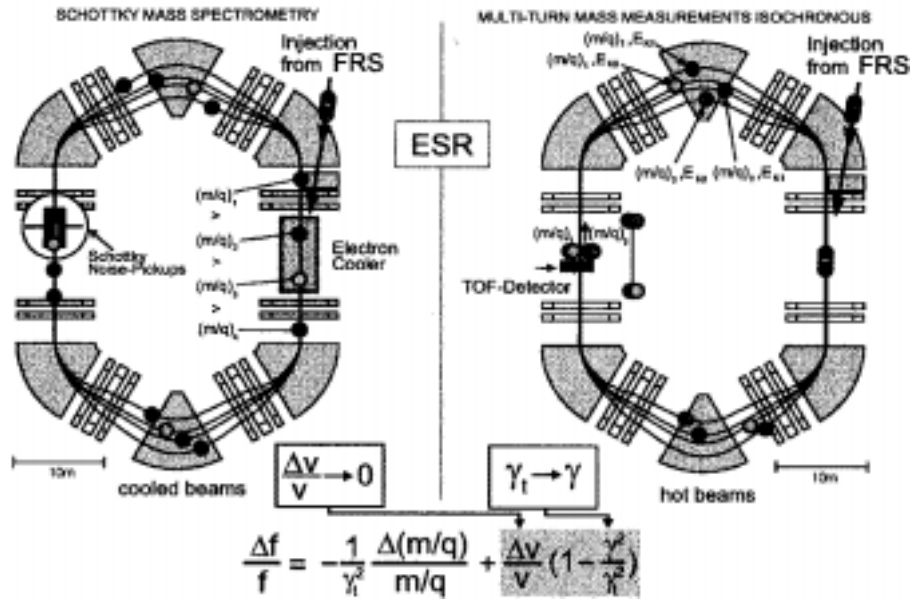


**Figure 3.** The mass resolution in a storage ring is given by the precision achieved for the frequency and velocity determination.  $\gamma$  is the relativistic Lorentz-factor and  $\gamma_t$  represents the reduced transition energy which characterizes the ion-optical mode of the ring. From this formula it is obvious that either cooling  $\Delta v/v \rightarrow 0$  or the isochronous condition,  $\gamma \rightarrow \gamma_t$ , are the basis of precise mass measurements.

### 3. Schottky mass measurements with cooled fragments

A production target of 8 g/cm<sup>2</sup> beryllium was placed at the entrance of the FRS. The target was especially chosen to inject a large number of elements and isotopes at the same time in the ESR. The incident energy was 930 MeV/u in the case of <sup>209</sup>Bi and 750 MeV/u in the case of <sup>58</sup>Ni-projectiles. These energies were selected to operate the electron cooler in the range of 200 kV for the terminal voltage. The fragments were separated with the FRS by pure magnetic rigidity ( $B\rho$ ) analysis during the major part of the mass measurements. In this case up to 60 different fragments were injected into the ESR by a single bunch of projectiles from SIS. In the ESR the ions were stored and cooled and detected via Schottky spectrometry.

Schottky spectroscopy is a widely used tool for beam diagnosis in circular accelerators and storage rings. The induced signals of the stored circulating ions in non-destructive Schottky noise-pickups (see left part of figure 3) are recorded and analysed.

Already in our pilot experiments with cooled projectile fragments [4,12] we have applied Schottky diagnostics and since then we have gradually developed this technique for the requirements of precision mass spectrometry [6,13,11]. The stored and cooled ions circulate in the ESR with revolution frequencies of about 1.9 MHz. In the experiments

we used the Schottky-noise signal of the 16th and the 32nd harmonic of the revolution frequencies. This high-frequency band has to be reduced by an admixture of an external oscillator frequency to match the working range of 100 kHz of the Fourier-analyser system. A data-acquisition system digitizes the Schottky signals with a sampling rate of 256 kHz. The frequency bandwidth of 100 kHz covers most of the  $B\rho$  acceptance of the stored beam in the ESR. The energy of our secondary beams ( $E_{\text{sec}} \approx 350$  MeV) allowed an optimum performance of the electron cooler and, in addition, presented the opportunity to measure the masses of bismuth fragments in bare, H-like, and He-like charge states. The mass measurement in different charge states yields not only redundant data for the same isotope, but is also an excellent feature for the calibration: Exotic neutron deficient nuclei having small magnetic rigidities and unknown masses appear in the Schottky spectra e.g. in He-like charge states in the neighborhood of isotopes with known masses in bare charge states located nearer to the  $\beta$  stability-line. The uncertainty of the rest mass of the electron and its binding energies are known with an error which is completely negligible compared to our present errors for the nuclear masses [6] being in the order of  $10^{-6}$ .

### *3.1 Results of the first Schottky mass measurements with bismuth-projectiles*

After having demonstrated that the results obtained with our novel experimental methods for direct mass measurements agree well with already known light masses [4,12], a large number of isotopes with unknown masses has been measured (figure 4).

The masses were evaluated by application of a maximum likelihood method. The relation of the mass-over-charge ratio as a function of the revolution frequency was fitted by a first-order polynomial connecting the known masses as references [14]. The unknown masses were determined by searching the maximum of the probability density for all data. The total error of the new masses is in the range of 100 to 200 keV, where a systematic error of about 95 keV has been included. The systematic error has been evaluated by a comparison with previously well-known masses. The good accuracy of our measured data is a solid basis for a better understanding of nuclear forces.

Figure 4 shows one proton separation energies for nuclei in the sub-uranium region. For several elements (Bi to Pa) we can derive mass values for nuclei with negative proton separation energies, i.e. the proton dripline could be located here. For other nuclei (Au to Ho) the location of the dripline can now be interpolated more precisely. The fact that we did not derive negative proton separation energies for even nuclei shows that the proton pairing energy plays an important role for dripline nuclei. Figure 5 shows that the proton pairing energy increases in direction towards the dripline. It is also worthwhile to mention that some of the neutron deficient mercury isotopes show an increase in their pairing energies compared to the neighboring isotopes (see also figure 4: large odd-even staggering for these isotopes). This may be an indication for shape coexistence in these nuclei [16].

In the last decades a large number of mass models have been proposed and developed [15]. They are based on different assumptions and can roughly be divided into three categories. They belong either to pure microscopic models, which start from the nucleon–nucleon interaction, or they belong to the macroscopic–microscopic models which use the liquid drop model with shell corrections or they are based on special mass relations combining the masses for adjacent nuclei. Here it is only the intention to give representative examples of different approaches to mass formulae. The most crucial test for the reliability

of a mass model is its predictive capability in new regions that were not considered when the theory was formulated.

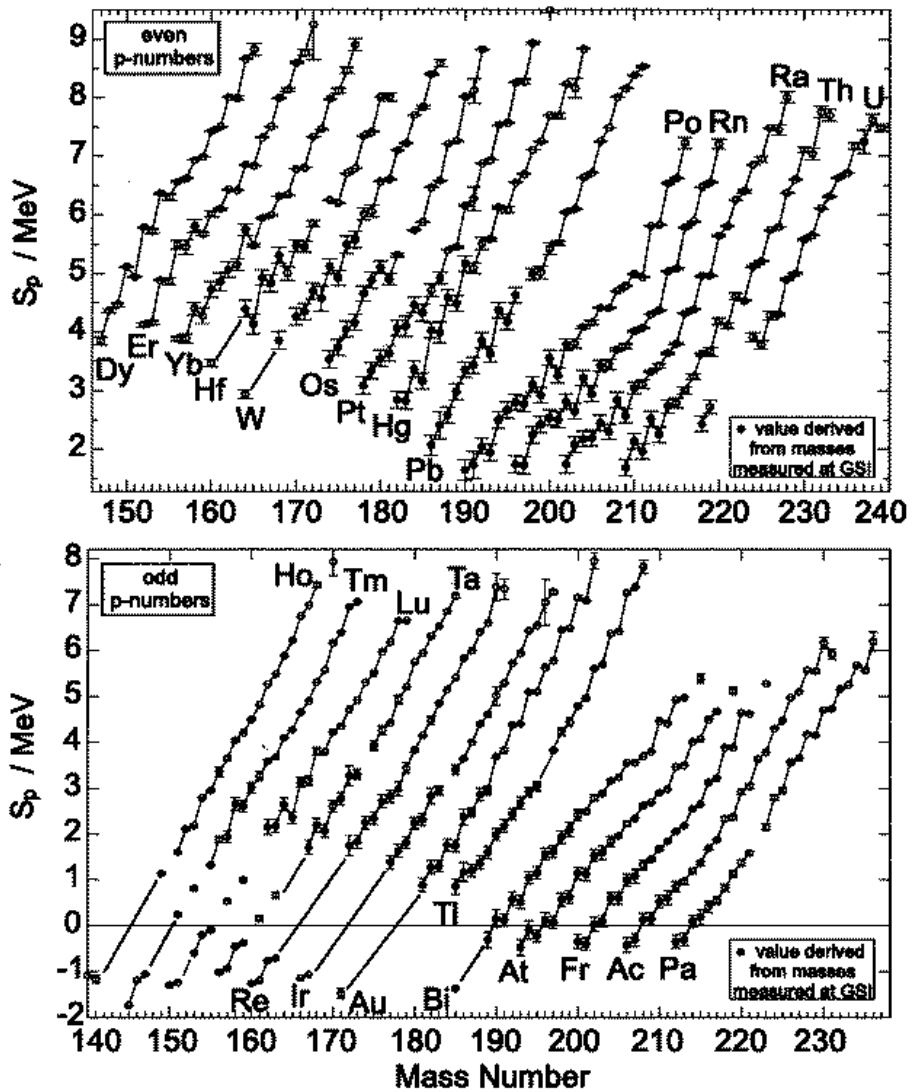
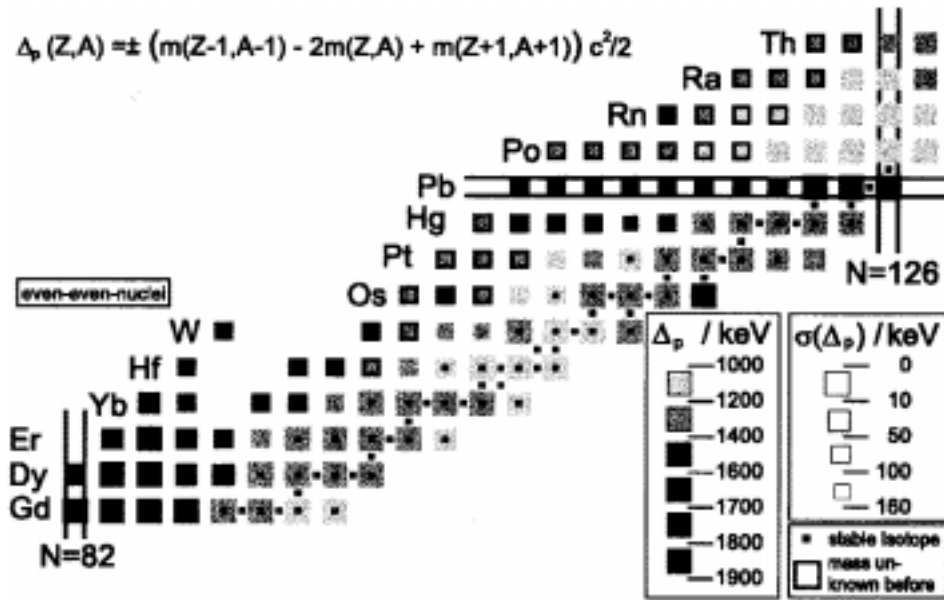


Figure 4. One proton separation energies for even (upper panel) and odd (lower panel) proton numbers. Masses derived from measurements at GSI are marked by a filled symbol.



**Figure 5.** Proton pairing energies for even–even nuclei. The strength of the proton pairing energy  $\Delta_p$  is given by the color of the squares representing one nucleus and the error  $\sigma(\Delta_p)$  is given by the size of the squares. Masses derived from measurements at GSI are marked with a frame. The formula used is not valid to show pairing energies for the lead isotopes, as it also exhibits the larger shell effect here.

**Table 1.** Mass models compared to our measured data (previously unknown values only). A  $\chi^2$ -test (eq.(1)) and a root mean square deviation (eq.(2)) from our data were calculated to compare with various types of models.

Mass formula	Category	$\chi^2$	$\sigma_{\text{rms}}$
Aboussir, Pearson <i>et al</i> [17]	microscopic (global)	60.5	773
Duflo–Zucker [18]	microscopic (global)	42.0	650
Möller–Nix [19]	macro-microscopic	40.3	644
Spanier–Johansson [20]	liquid drop with corr. (global) contributions (local)	143.5	1190
Jänecke–Masson [21]	mass relations (local)	20.5	467
Audi–Wapstra <i>et al</i> [14]	least-squares adjustment	1.8	137

Using our new mass values we can check the predictive power of various mass formulae tested by the following  $\chi^2$ -criterion.

$$\chi^2 = \frac{1}{n-1} \sum_{i=1}^n \frac{(M_{\text{exp}} - M_{\text{th}})_i^2}{(\Delta M_{\text{exp}})_i^2}, \quad (1)$$

where  $n$  is the number of the compared nuclei.  $M_{\text{exp}}$  and  $M_{\text{th}}$  represent the measured masses and the theoretically determined masses respectively.

To compare a model to experimental data disregarding error bars the classical rms deviation is used:

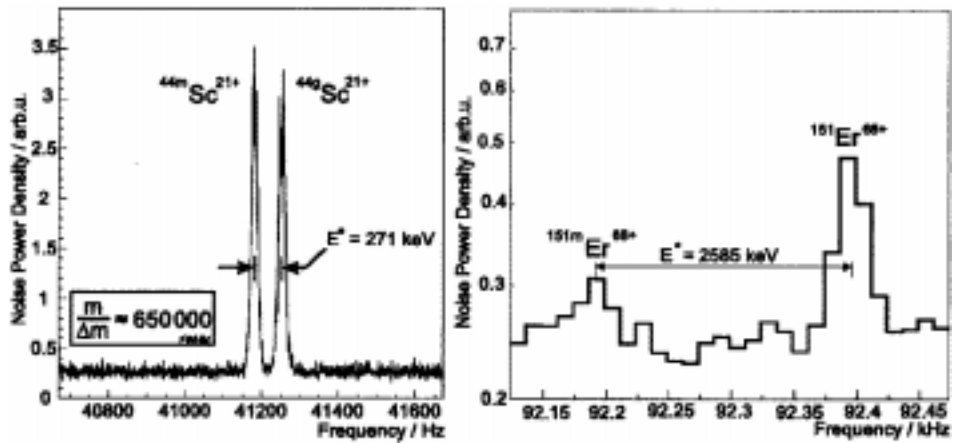
$$\sigma_{\text{rms}}^2 = \frac{1}{n-1} \sum_{i=1}^n (M_{\text{exp}} - M_{\text{th}})_i^2. \quad (2)$$

Table 1 shows various mass models and mass extrapolations including their predictive power for our 193 previously unknown masses according to eqs (1) and (2). One may easily see from table 1 that these mass models do not predict new masses with a precision needed for a good understanding of the mass surface and to accurately predict the positions of driplines. The extrapolations of Audi and Wapstra [14] however give a satisfactory result for our recently measured masses.

### 3.2 Experimental improvements for Schottky mass measurements

A number of important improvements could be achieved in our recent experiment in 1997. The performance of the ESR cooler was considerably improved yielding a much stronger cooling force and better stability which led to shorter cooling times and, therefore, gave access to isotopes with shorter half-lives. The maximum voltage of the cooler could also be improved so that we were able to access nuclei with lower proton numbers compared to the 1995 measurements using the same projectile. Furthermore, a better stabilization of the power supplies and an improved magnetic field homogeneity of the ESR magnets helped to significantly improve the resolving power in the mass spectra.

In figure 6 we present Schottky frequency spectra for bismuth and nickel fragments characterized by a mass resolving power of  $6.5 \cdot 10^5$  which is about a factor of two better than in our experiment performed in 1995 [6]. It should be mentioned that the half-life



**Figure 6.** Mass resolved Schottky frequency spectra of bare  $^{44g,m}\text{Sc}$  ions (ground and isomeric states separated by 271 keV, left panel) of bare  $^{151g,m}\text{Er}$  ions (ground and isomeric states separated by 2585 keV, right panel) [7].

of neutral  $^{151m}\text{Er}$  atoms is 0.58 s, however, in our case with bare nuclei the half-life is prolonged by roughly a factor of 21. In the experiment performed in 1997 we used  $^{58}\text{Ni}$  and  $^{209}\text{Bi}$  projectiles and set the magnetic fields of the FRS and ESR and the cooler voltage corresponding to a constant  $B\rho$  value of 6.5 Tm. The advantage of this procedure was that we only had to adjust the ESR once to the FRS which turned out to be a crucial part in the measurements performed in 1995. The scaling of the incident energy (750–900 MeV/u) was a faster procedure to fill the ESR with the desired exotic nuclei.

A new data acquisition system was taken into operation which represented further experimental improvements. The digitized signals of the Schottky pick-up were sequentially recorded on tape giving a time stamp of every event. Fast Fourier transformation of this time-correlated data can be performed off-line in order to obtain the revolution frequencies of the stored ions as well as the half-life information of the radioactive species. Furthermore, time-drifts of the experimental conditions can be corrected in the off-line analysis.

#### 4. Isochronous mass measurements with projectile fragments

There are still regions on the chart of nuclei where Schottky mass spectrometry can still contribute to an improved knowledge of nuclear masses using e.g. stochastic cooling [22], but the most exotic nuclei have too short half-lives for this experimental technique. Exotic nuclei with half-lives shorter than the time needed for cooling and recording can be investigated by time-of-flight techniques in the ESR. Here the ESR is operated in the isochronous mode [23,24]. In this case, the magnetic fields of the ESR are set such that the revolution frequency of an ion species becomes independent of its velocity spread (see right panel of figure 3). This novel experimental technique has been successfully applied in first measurements with nickel [24] and neon fragments. The ESR lattice was tuned to  $\gamma_t=1.37$  corresponding to a kinetic energy of 345 MeV/u for the stored ions.  $\gamma_t$  is mainly determined by the dispersion function inside the dipole magnets. First frequency spectra were recorded in the isochronous mode using projectile fragments created by a  $^{58}\text{Ni}$  beam. The relative velocity spread of these stored ions was about  $10^{-3}$ . Although the momentum acceptance inside the ESR is strongly reduced in the isochronous mode, as compared to the standard operation, the measured  $m/q$  acceptance still reached 1.2%. Already in this pilot experiment we achieved a remarkable mass resolving power of  $m/\Delta m = 1.5 \cdot 10^5$  (FWHM) as demonstrated by resolving  $^{56}\text{Ni}$  and  $^{52}\text{Fe}$  fragments (see [7]). Mass uncertainties for nickel-fragments were found to be in the order of 30–60 keV. In another experiment with a  $^{22}\text{Ne}$ -beam cooling was applied in addition to measure the revolution frequency of the fragments circulating in the isochronous lattice of the ESR. As a consequence very small linewidths of the frequency peaks were derived which led to mass accuracies below 10 keV for Ne-fragments. Applying cooling to isochronous beams gives the possibility to nicely map  $\gamma_t$  as a function of the pathlength. It was found that a linear mass calibration can be used over a large frequency range. In the off-line analysis the measured dependence of the frequency on the velocity could be well understood and was reproduced by ion-optical model calculations. New ion-optical calculations suggest strong improvements for the isochronous mode which will be tested in coming experiments [25]. For the future it is planned to perform direct mass measurements of  $^{238}\text{U}$  fission fragments ( $T_{1/2} < 1$  s) using the isochronous method.

## References

- [1] H-J Kluge, in [15]
- [2] G Audi, O Bersillon, J Blachot and A H Wapstra, *Nucl. Phys.* **A624**, 1 (1997)
- [3] W Mittig, A Lepine-Szily and N A Orr, *Ann. Rev. Nucl. Sci.* **47**, 27 (1997)
- [4] H Geissel et al, *Phys. Rev. Lett.* **68**, 3412 (1992)
- [5] B Franzke et al, *Nucl. Instrum. Methods* **B24/25**, 18 (1987)
- [6] T Radon, Th Kerscher and B Schlitt et al, *Phys. Rev. Lett.* **78**, 4701 (1997)
- [7] H Geissel and T Radon et al, Experiments with Stored Relativistic Exotic Nuclei in CP455, *ENAM 98: Exotic Nuclei and Atomic Masses* edited by B M Sherril, D J Morrissey, and Cary N Davids (The American Institute of Physics, 1-56396-804-5/98, 1998)
- [8] K Blasche and B Franzczak, *Proc. of the third European Part. Acc. Conf., Berlin* edited by H Henke, H Homeyer and Ch Petit-Jean-Genaz (Gif-sur-Yvette: Editions Frontière, 1992) p. 9
- [9] H Geissel, et al, *Nucl. Instrum. Methods* **B70**, 286 (1992)
- [10] M Steck et al, *Phys. Rev. Lett.* **77**, 3803 (1996)
- [11] B Schlitt et al, *Hyp. Int.* **99**, 117 (1996); *Nucl. Phys.* **A626**, 315c (1997)
- [12] H Irnich, H Geissel and F Nolden et al, *Phys. Rev. Lett.* **75**, 4182 (1995)
- [13] B Franzke et al, *Phys. Scr.* **T59**, 176 (1995)
- [14] G Audi and A H Wapstra, *Nucl. Phys.* **A595**, 409 (1995)
- [15] D Guillemaud-Mueller (ed.) *Proceedings of ENAM95* (Gif-sur-Yvette: Editions Frontière, ISBN 2-86332-186-2, 3, 1995)
- [16] G Ulm et al, *Z. Phys.* **A325**, 247 (1986)
- [17] Y Aboussir, J M Pearson, A K Dutta and F Tondeur, *Atomic Data Nucl. Data Tables* **61**, 127 (1995)
- [18] J Duflou and A P Zuker, *Phys. Rev.* **C52**, 23 (1995)
- [19] P Möller, J R Nix, W D Myers and W J Swiatecki, *Atomic Data Nucl. Data Tables* **59**, 185 (1995)
- [20] L Spanier and S E Johannson, *Atomic Data Nucl. Data Tables* **93**, 259 (1988)
- [21] J Jännecke and P J Masson, *Atomic Data Nucl. Data Tables* **39**, 265 (1988)
- [22] F Nolden, B Franzke and A Schwinn, GSI-Report 98-1 171 (1998)
- [23] H Wollnik et al, GSI-Report 86-1 372 (1986)
- [24] M Hausmann et al, GSI-Report 98-1 170 (1998)
- [25] M Hausmann et al, *Proc. of the 6th European Particle Accelerator Conference* edited by S Myers, L Liljeby, Ch Petit-Jean-Genaz, J Poole and K-G Rensfeldt (Institute of Physics Publishing, Bristol, 1998) pp. 511–513